https://www.scientificarchives.com/journal/journal-of-nanotechnology-and-nanomaterials

Journal of Nanotechnology and Nanomaterials Short Communication

Ligand-free Few Atoms Ag Nanoclusters Synthesis and Their Potential Application as Photocatalytic Agents

Jesica M. J. Santillán[1*], David Muñetón Arboleda[2], Diego Muraca[3], Daniel C. Schinca[1,4], Lucía B. Scaffardi[1*]

[1]Centro de Investigaciones Ópticas (CIOp), (CONICET - CIC - UNLP), Camino Centenario y 506, 1897 Gonnet, La Plata, Argentina

[2]Instituto de Investigaciones Fisicoquímicas Teóricas y Aplicadas (INIFTA), Diagonal 113 y 64 (CONICET-UNLP); on leave from CIOp

[3]Instituto de Física "Gleb Wataghin", Universidade Estadual de Campinas, Campinas, Brazil

[4]Facultad de Ingeniería, UNLP, 115 y 49, 1900 La Plata, Buenos Aires, Argentina

[*]Correspondence should be addressed to Lucía B. Scaffardi; lucias@ciop.unlp.edu.ar, Jesica M. J. Santillán; jesicas@ciop.unlp.edu.ar

Received date: August 25, 2020, **Accepted date:** September 17, 2020

Abstract

We have implemented ultrafast laser ablation synthesis in liquids together with mechanical centrifugation to obtain ligand-free silver nanoclusters (Ag NCs). Given the nature of this technique, the NCs colloids produced are highly pure which avoids additional cleaning protocols. The mechanical centrifugation of the colloids helps to separate the NCs from their larger counterparts (nanoparticles (NPs)), present in the suspension. Synthesized NC colloids are studied by fluorescence spectroscopy observing UV bands corresponding with HOMO-LUMO cluster transitions, and HRTEM measurements where Ag NCs clouds and Ag atomic clusters are observed. Finally, the photocatalytic response of the Ag NCs was studied by the degradation of the standard molecule Methylene Blue (MB) in interaction with white light. It was observed that when MB and Ag NCs are mixed in the solution, degradation of MB is much faster, indicating the strong photocatalytic response of NCs, even at low concentrations.

Introduction

Reducing the size of a metal from macroscopic to the nanoscale generates a scaling behavior in physical and chemical properties due to the large surface-to-volume fraction. While a further size reduction to small clusters under 2 nm (<~100 atoms) yield geometric and electronic structures which are still different from their nanoparticle (NP) counterpart [1]. These small clusters adopt special atomic arrangements to reduce their surface energy, and their electronic structures are no longer continuous, as in bulk metals, but rather discretized. Owing to these peculiar characteristics, metal clusters exhibit striking properties and characteristics which are dependent on the number of atoms present in them. For these reasons, small metal clusters have attracted much attention as new functional nanomaterials, which make them promising candidates for various applications in a wide range in the science and technology. Therefore, when working with these small metal clusters, the synthesis plays a very important role allowing expanding the range of applications. In the last years, numerous studies on chemical synthesis of these clusters have been reported [2-11]. Nevertheless, several of these methods that tend to yield highly monodisperse clusters suspensions, are mixed with unwanted chemical precursors, resulting in aggregation, background noise in analytical chemistry, toxicity, and deactivation of the catalyst. Thus, the interest in finding new routes of green synthesis to boost the catalytic and biomedical properties of small metal clusters has become an active branch of nanotechnology. For this purpose, ultrafast pulses laser ablation in liquids [12-16] is an alternative technique for synthesize metal NPs free of unwanted by-products.

In this work, we employed the physical method of ultrafast laser ablation of silver target in water, together with mechanical centrifugation to obtain ligand-free few-atoms silver nanoclusters (Ag NCs). Luminescence

spectral behavior of the obtained colloids was observed by fluorescence spectroscopy and was analyzed using the Jellium model to characterize the HOMO-LUMO energy band gap of few atoms NCs. Also, HRTEM measurements were made confirming the presence of Ag NCs and small NPs. Finally, photocatalytic efficiency of the NCs was analyzed through degradation of Methylene Blue (MB) together with highly centrifuged colloid, showing an enhanced photocatalytic activity compared with pure MB. The results presented here are complementary to those recently published [17].

Materials and Methods

Ligand-free Ag colloidal suspensions were synthesized using a 120 fs pulse width Ti:Sapphire chirped pulse amplification system (Spectra Physics), centred at 800 nm wavelength, 1 kHz repetition rate and a maximum output pulse energy of 1 mJ. A solid Ag disk (99.99 % purity grade) of a 1 cm diameter and 0.1 cm thick, placed at the bottom of a beaker filled with 2 mL of Milli-Q water was used as ablation target.

Mechanical centrifugation was implemented to achieve the separation of the small NCs from the NPs of larger sizes present in the obtained colloids. Fluorescence response of the as- prepared colloids and supernatant of the centrifuged colloids was obtained using a Shimadzu RF- 5301PC spectrofluorophotometer in the range 200 nm to 700 nm, to different centrifugation conditions that were carefully monitored controlling time and speed. The excitation wavelength employed was 220 nm.

The photocatalytic activity of the Ag NCs was performed by monitoring the degradation of a mixture of MB with the supernatant of the centrifuged colloids for 1000 min at 15000 rpm as compared to a pure MB solution (0.04 mM), when they were illuminated with a white light lamp. The degradation was measured through the absorption spectra obtained using a Shimadzu UV-1650PC spectrophotometer in the wavelength range of 300 nm to 900 nm, taken at fixed time intervals.

Results and Discussion

Given the bottom-up nature of femtosecond laser ablation synthesis, colloids obtained from a Ag target in liquids by this technique present, in general, NPs between 2 and 20 nm together with structures of a few and a few tens of atoms. The latter present radiative transitions (fluorescence) and not a plasmonic resonance band like the larger NPs. For this reason, UV- visible fluorescence spectroscopy measurements using an excitation beam of 220 nm were carried out. To obtain luminescence information as a function of the excitation energy, the recorded fluorescence spectra are normalized to the absorbance of the sample in λ= 220 nm. Figure 1a exhibits a typical fluorescence spectrum of a colloid synthesized by 600 μJ pulse energy fs laser ablation. Three peaks around 284 nm, 330 nm and 358 nm, besides a notorious broad fluorescence band from 400 nm to 625 nm are observed. The peak at 220 nm corresponds to the scattering of the excitation light. This spectral behavior of the luminescence of metallic nanostructures is due to further confinement to smaller sizes than Fermi wavelength of an electron (0.7 nm approximately) which should result in discrete, quantum-confined electronic transitions [18]. This phenomenon has been studied in the light of the Jellium model, in which the electronic dynamics of metallic structures of few atoms are analyzed, considering the electrons as a free gas with negative charge moving in a weakly attractive mean field created by positively charged ionic cores with symmetric spherical 3D harmonic potential. The Jellium model predicts that, for this type of structure, the HOMO-LUMO transitions energy depends on the Fermi energy and the number of atoms, $E_g = E_F \cdot N^{-x}$, where $x = \frac{1}{3}, \frac{2}{3}$ for multi- and single-electron transitions, respectively [19,20]. Particularly Zheng et al. [21] found that in the case of $x = \frac{1}{3}$, the equation $Eg = E_F \cdot N^{-1/3}$ describes the experimental results of electronic transitions such as those observed in Figure 1a. While the case of $x = \frac{2}{3}$ is related to the transitions of semiconductor quantum dots [22].

From the aforementioned equation, the number of atoms of the NCs in solution can be determined, measuring the bandgap energy E_g from the peak wavelength of the experimental fluorescence UV-visible spectrum, considering E_F = 5.49 eV [23]. Figure 1b shows in full line the E_g dependence on N, while triangles indicate E_g of the clusters present in the colloid. It can be seen that they lay on the line that represents the general decreasing dependence on cluster atoms number.

Clusters with 2, 3 and 4 atoms (Ag_2, Ag_3 and Ag_4) correspond to the first three recorded distinct peaks in Figure 1a, while peaks corresponding to Ag_7, Ag_8, Ag_9, Ag_{10} and Ag_{11} form the rising side and maximum of the wide experimental band. Besides, Ag_{12} to Ag_{20} bands that are overlapped, forming the falling side of the wide band in Figure 1a. The E_g values of these latter bands are indicated by circles in Figure 1b. From a side-view, a 30 s exposure image (inset) shows the blue-reddish fluorescence corresponding to the wide fluorescence band centered around 480 nm, which can be seen even with the naked eye.

Table 1 summarizes peak wavelength (λ), E_g and N for the different clusters found in the obtained colloidal suspensions. It is worth noticing that, according to the relation between band gap energy and atoms number, the

spectrofluorophotometer wavelength range would allow us to see fluorescence of Ag NCs of up to N = 30 atoms (Ag_{30}). However, in our case, using fs laser ablation we observed clusters only up to 20 atoms, as can be observed in Figures 1a and 1b and Table 1.

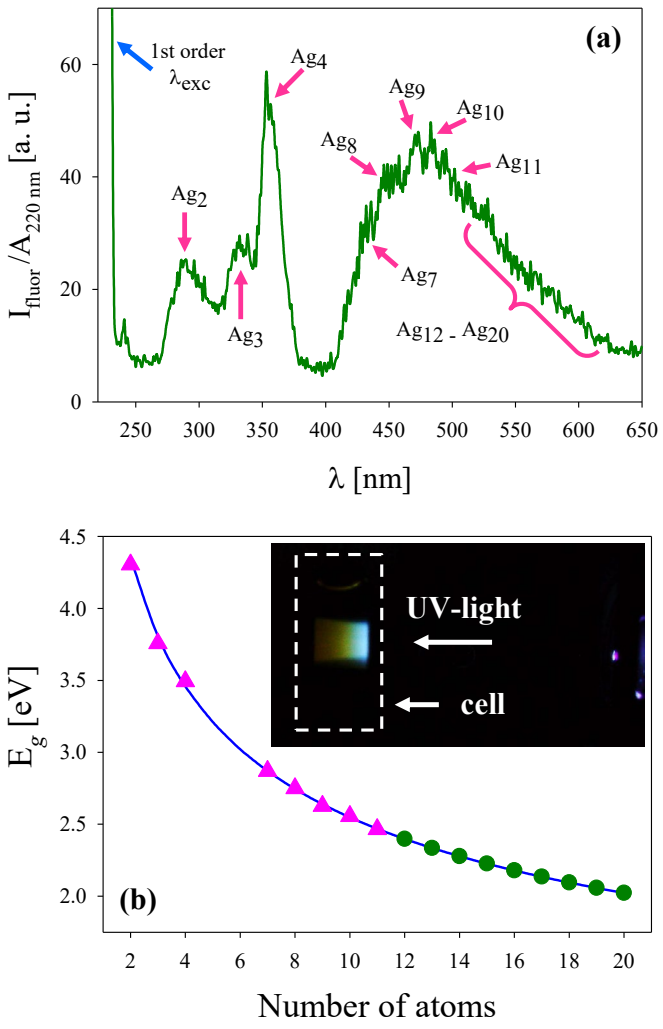

Figure 1: (a) Fluorescence spectrum in the UV-visible wavelength range exhibits noticeable peaks corresponding to Ag_2, Ag_3 and Ag_4 clusters together with the wide band between 400 nm and 625 nm [17]. Arrows in the wide band indicate the wavelengths corresponding to Ag_7 to Ag_{11} NCs, while Ag_{12} to Ag_{20} is indicated by the curly bracket. **(b)** E_g vs number of atoms (N) according to the jellium model (full line). Triangles denote observed experimental fluorescence band peaks. Circles denote the gap energy of Ag_{12} to Ag_{20} clusters included in the right of the wide band. Inset shows a side-view 30 s exposure image of the sample recorded under the same conditions used during the fluorescence spectroscopy measurements.

λ (nm)	E_g (eV)	N
284.5 ± 0.5	4.357 ± 0.007	2
325.7 ± 0.5	3.806 ± 0.005	3
358.5 ± 0.5	3.458 ± 0.004	4
432.0 ± 0.5	2.869 ± 0.003	7
451.7 ± 0.5	2.745 ± 0.003	8
469.8 ± 0.5	2.639 ± 0.003	9
486.6 ± 0.5	2.548 ± 0.002	10
502.3 ± 0.5	2.468 ± 0.002	11
517.1 ± 0.5	2.398 ± 0.002	12
531.0 ± 0.5	2.334 ± 0.002	13
544.3 ± 0.5	2.277 ± 0.002	14
557.0 ± 0.5	2.226 ± 0.002	15
569.1 ± 0.5	2.178 ± 0.002	16
580.7 ± 0.5	2.135 ± 0.002	17
591.9 ± 0.5	2.094 ± 0.001	18
602.6 ± 0.5	2.057 ± 0.001	19
613.0 ± 0.5	2.022 ± 0.001	20

Table 1: Peak wavelength (λ), energy gap (Eg) and clusters atom number (N) present in the colloidal suspension generated by femtosecond laser ablation.

To confirm the presence of the NCs in the obtained colloids, HRTEM images were acquired employing HAADF-STEM mode to acquire better quality images (see [17] for more clear evidence of clusters formation). Figure 2 presents NCs and NPs in several nucleation stages. In both panels of Figure 2 Ag NPs can be observed in a range of approximately 1.7 nm to 3.1 nm in size, some of them with noticeable crystalline structures (pointed with arrows). In addition, there are present some "clouds" of NCs (solid yellow circles) and few atoms Ag NCs (dashed blue circles) coexisting with the small NPs. These HRTEM images are in agreement with the results obtained by fluorescence spectroscopy of the as-prepared colloid (Figure 1) and the absorbance spectra behavior that will be shown later in Figure 4.

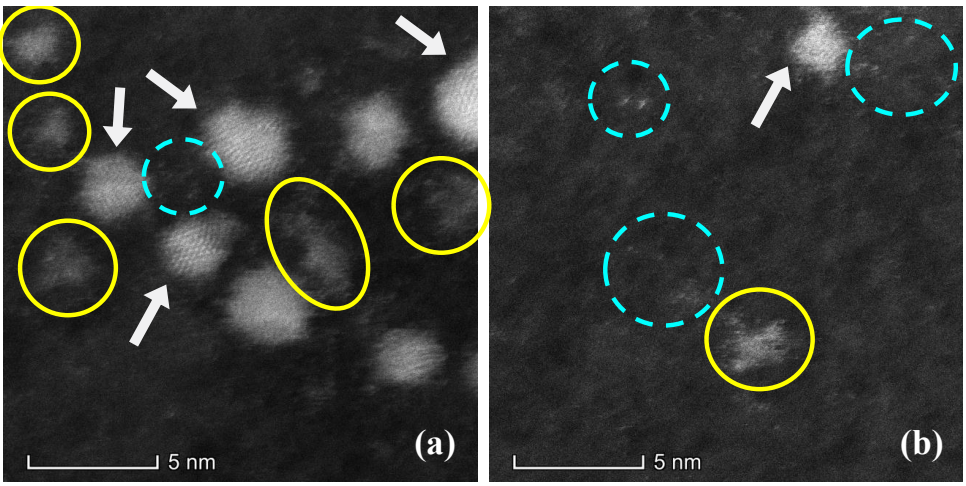

Figure 2: HRTEM images acquired with HAADF-STEM mode show the presence of Ag NPs with crystalline structure (pointed by arrows), "clouds" of Ag NCs (enclosed by solid yellow circles) and few atoms Ag NCs (enclosed by dashed circles).

After carefully trying different centrifugation speeds and times, it was found that upon reaching centrifugation with 15000 rpm, the intensity of the fluorescence bands at 284 nm and 330 nm increases significantly with respect to the 360 nm band, which means that the smaller NCs (Ag_2 and Ag_3) remain mainly in the supernatant.

Figure 3 presents the fluorescence spectra of the colloid centrifuged with 15000 rpm during different times. Inset shows an enlargement of the as-prepared and 20 min centrifuged colloids are shown together with water spectrum to comparison.

It can be observed the fluorescence bands corresponding to Ag_2, Ag_3 and Ag_4 NCs progressively increase as centrifugation time increases, with a noticeable predominance of Ag_2 and Ag_3 overlapped bands. This fact is due to the gradual decreasing of Ag NPs presence in the colloid that quench the luminescence produced by the NCs. The above is explained because the Ag NPs plasmonic absorbance is close to the HOMO-LUMO NCs emission.

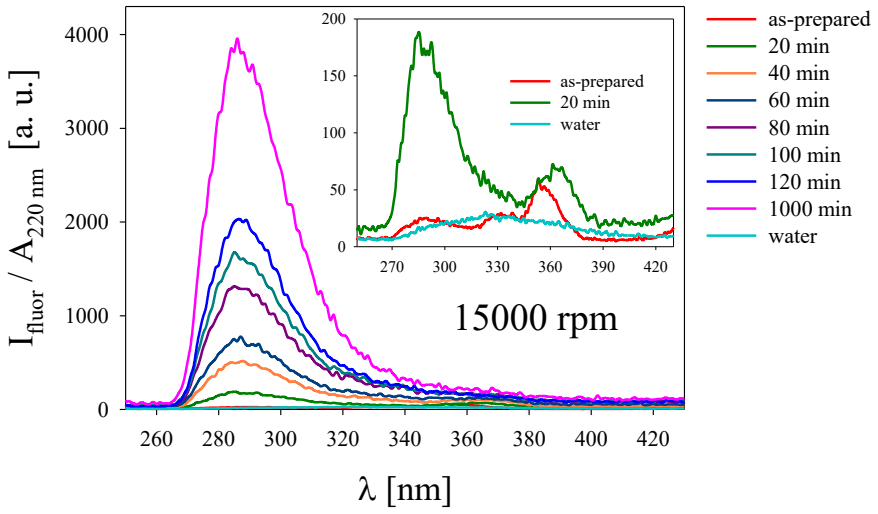

Figure 3: Fluorescence spectra of the Ag colloids after different centrifugation times with 15000 rpm. Inset shows spectra of the as-prepared and 20 min centrifugation colloids as well as that for pure water for comparison [17].

Regarding the photocatalysis studies of Ag NCs, different authors have dedicated themselves to this task, carrying out proofs-of-concept with very good results in the degradation of acridine red [24], formic acid [25], among others. However, not enough studies have been developed in Ag NCs with absence of capping such as those obtained by femtosecond laser ablation. To analyze the photocatalytic response of the Ag NCs, a control of the degradation of a MB solution (0.04 mM) in a mixture with a colloid after synthesized and centrifuged for 1000 min at 15000 rpm, was carried out. This control was performed monitoring periodically the absorption spectra by means of UV-visible spectrophotometer. Panel (a) of Figure 4 presents the absorption spectra of the pure MB solution for different times while illuminated with a white lamp. In these spectra it is possible to observe the decrease in the intensity of the absorption as time passes, indicating the native degradation of the dye molecule due to the effect of white light.

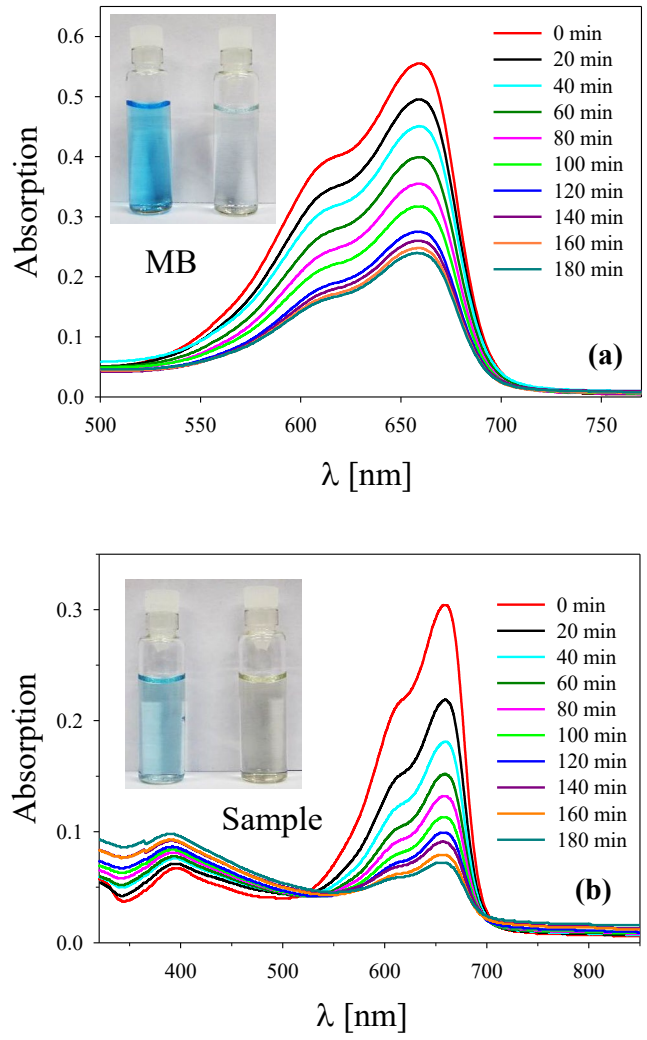

Figure 4: Monitoring of photocatalytic degradation of MB illuminated by a white light lamp recorded at fixed time intervals. Absorption spectra: (a) pure MB and (b) mixture of MB with centrifuged Ag colloid (sample) [17].

In contrast, panel (b) exhibits the photocatalytic degradation of the MB solution when it is mixed with the centrifuged Ag colloid to 1000 min (containing a lesser amount NPs and the larger sized NCs), under the action of the same white light lamp. It is seen that the absorbance peak decreases progressively faster than for the case of pure MB solution, also characteristic silver plasmon absorbance is present indicating the presence of small Ag NPs. Inspection of the time evolution of the absorbance band at 660 nm in Figure 4 suggests that dye photobleaching gets stronger from pure MB to sample. The insets in Figure 4 show a picture where the discoloration after photocatalytic degradation in both samples is observed.

The photocatalytic degradation of MB and the sample (mixture of MB and centrifuged Ag colloid) was quantitative determined by the expression:

$$\text{Photocatalytic degradation (\%)} = 100 \times (A_o - A_t)/A_o$$

Figure 5 shows the calculated values of the photocatalytic degradation (in %) for the pure MB solution and sample (MB + NCs).

As observed in Figure 5, the photocatalytic degradation of the pure MB reaches to 57% after 3 h of illumination, while the sample reaches 79%. Despite of their low concentration in the sample, the Ag NCs synthetized present an evident photocatalytic action, making it a possible photocatalyst agents in different applications.

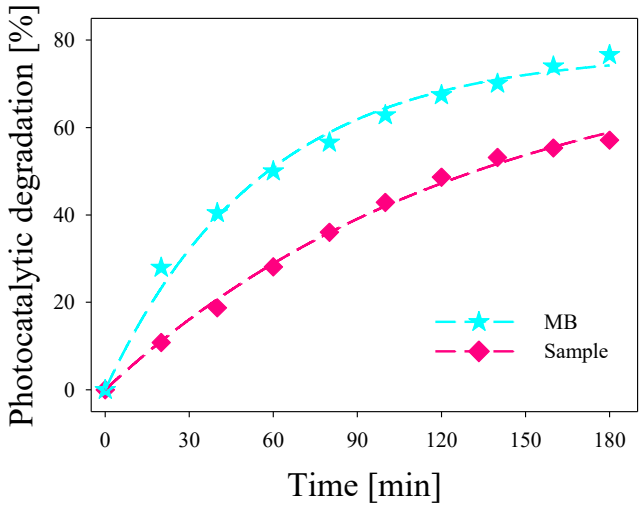

Figure 5: Experimental photocatalytic degradation for pure MB and sample calculated from data shown in Figure 4 [17].

Conclusion

In summary fs pulse laser ablation in liquids together with mechanical centrifugation allow obtaining ligand free few atoms Ag NCs. UV-visible fluorescence spectroscopy of the colloids reveal several peaks attributed to the HOMO-LUMO electronic transitions of few atom NCs by the Jellium model. On the other hand, HRTEM analysis showed the presence of NCs in different aggregation stages, as atomic cluster agglomerations and clouds of free-standing NCs.

Photocatalytic activity of Ag colloidal suspension was assessed by degradation of MB solution and a mixture of this with a freshly prepared Ag NCs. The results showed that in the presence of NCs the MB solution has a degradation 22% greater than its native photocatalysis. This proves that, even at low concentrations, Ag NCs show strong photocatalytic activity.

Acknowledgements

We thank C2NANO-Brazilian Nanotechnology National Laboratory (LNNano) at Centro Nacional de Pesquisa em Energia e Materiais (CNPEM)/MCT (Research Proposals #16976, #19927 and #22345) and FAPESP 17/10581-1, Brasil. This work was Granted by PIP 0280 of CONICET, MINCyT-PME 2006-00018, 11/I197, Facultad de Ingeniería of Universidad Nacional de La Plata and PICT 2016-3205 of Agencia Nacional de Promoción Científica y Tecnológica, MinCyT, Argentina. Fabrication of NPs by Ultrafast Pulse Laser Ablation were carried out at CIOp (CONICET, CICBA and UNLP), La Plata.

References

1. Corain B, Schmid G, Toshima N, editors. Metal nanoclusters in catalysis and materials science: the issue of size control. Amsterdam: Elsevier; 2007.

2. Santiago Gonzalez B, Rodríguez MJ, Blanco C, Rivas J, López-Quintela MA, Martinho JM. One step synthesis of the smallest photoluminescent and paramagnetic PVP-protected gold atomic clusters. Nano Letters. 2010 Oct 13;10(10):4217-21.

3. Buceta D, Piñeiro Y, Vázquez-Vázquez C, Rivas J, López-Quintela MA. Metallic clusters: theoretical background, properties and synthesis in microemulsions. Catalysts. 2014 Dec;4(4):356-74.

4. Rivas J, García-Bastida AJ, López-Quintela MA, Ramos C. Magnetic properties of Co/Ag core/shell nanoparticles prepared by successive reactions in microemulsions. Journal of Magnetism and Magnetic Materials. 2006 May 1;300(1):185-91.

5. Wu S, Zeng H, Schelly ZA. Growth of uncapped, subnanometer size gold clusters prepared via electroporation of vesicles. The Journal of Physical Chemistry B. 2005 Oct 13;109(40):18715-8.

6. González BS, Blanco MC, López-Quintela MA. Single step electrochemical synthesis of hydrophilic/hydrophobic Ag 5 and Ag 6 blue luminescent clusters. Nanoscale. 2012;4(24):7632-5.

7. Vilar-Vidal N, Blanco MC, Lopez-Quintela MA, Rivas J, Serra C. Electrochemical synthesis of very stable photoluminescent copper clusters. The Journal of Physical Chemistry C. 2010 Sep 30;114(38):15924-30.

8. Donkers RL, Lee D, Murray RW. Synthesis and isolation of the molecule-like cluster Au38 (PhCH2CH2S) 24. Langmuir. 2004 Mar 2;20(5):1945-52.

9. Jin R, Zeng C, Zhou M, Chen Y. Atomically precise colloidal metal nanoclusters and nanoparticles: fundamentals and opportunities. Chemical Reviews. 2016 Sep 28;116(18):10346-413.

10. Yao Q, Yuan X, Chen T, Leong DT, Xie J. Engineering functional metal materials at the atomic level. Advanced Materials. 2018 Nov;30(47):1802751.

11. Wu Z, Yao Q, Zang S, Xie J. Directed self-assembly of ultrasmall metal nanoclusters. ACS Materials Letters. 2019 Jul 2;1(2):237-48.

12. Amendola V, Amans D, Ishikawa Y, Koshizaki N, Scirè S, Compagnini G, et al. Room-temperature laser synthesis in liquid of oxide, metal-oxide core-shells and doped oxide nanoparticles. Chemistry–A European Journal. 2020 Apr 20; 26: 9206–9242.

13. Zhu L, Gharib M, Becker C, Zeng Y, Ziefuß AR, Chen L, et al. Synthesis of Fluorescent Silver Nanoclusters: Introducing Bottom-Up and Top-Down Approaches to Nanochemistry in a Single Laboratory Class. Journal of Chemical Education. 2019 Nov 5;97(1):239-43.

14. Arboleda DM, Santillán JM, Arce VB, van Raap MB, Muraca D, Fernández MA, et al. A simple and "green" technique to synthesize long-term stability colloidal Ag nanoparticles: Fs laser ablation in a biocompatible aqueous medium. Materials Characterization. 2018 Jun 1;140:320-32.

15. Santillán JM, Arboleda DM, Coral DF, van Raap MB, Muraca D, Schinca DC, et al. Optical and magnetic properties of fe nanoparticles fabricated by femtosecond laser ablation in organic and inorganic solvents. ChemPhysChem. 2017 May 5;18(9):1192-209.

16. Muñeton Arboleda D, Santillán JM, Mendoza Herrera LJ, van Raap MB, Mendoza Zelis P, Muraca D, et al. Synthesis of Ni nanoparticles by femtosecond laser ablation in liquids: structure and sizing. The Journal of Physical Chemistry C. 2015 Jun 11;119(23):13184-93.

17. Santillán JM, Arboleda DM, Muraca D, Schinca DC, Scaffardi LB. Highly fluorescent few atoms silver nanoclusters with strong photocatalytic activity synthesized by ultrashort light pulses. Scientific Reports. 2020 May 19;10(1):1-3.

18. De Heer WA. The physics of simple metal clusters: experimental aspects and simple models. Reviews of Modern Physics. 1993 Jul 1;65(3):611.

19. Kreibig U, Vollmer M. Optical Properties of Metal Clusters; Springer-Verlag: Berlin, 1995.

20. Bonatsos D, Lenis D, Raychev PP, Terziev PA. Deformed harmonic oscillators for metal clusters: Analytic properties and supershells. Physical Review A. 2002 Feb 14;65(3):033203.

21. Zheng J, Zhang C, Dickson RM. Highly fluorescent, water-soluble, size-tunable gold quantum dots. Physical Review Letters. 2004 Aug 13;93(7):077402.

22. Brus LE. Electron–electron and electron-hole interactions in small semiconductor crystallites: The size dependence of the lowest excited electronic state. The Journal of Chemical Physics. 1984 May 1;80(9):4403-9.

23. Santillán JM, Videla FA, van Raap MF, Muraca D, Scaffardi LB, Schinca DC. Influence of size-corrected bound-electron contribution on nanometric silver dielectric function. Sizing through optical extinction spectroscopy. Journal of Physics D: Applied Physics. 2013 Oct 1;46(43):435301.

24. Samai B, Chall S, Mati SS, Bhattacharya SC. Role of silver nanoclusters in the enhanced photocatalytic activity of cerium oxide nanoparticles. European Journal of Inorganic Chemistry. 2018 Jul 23;2018(27):3224-31.

25. El-Roz M, Telegeiev I, Mordvinova NE, Lebedev OI, Barrier N, et al. Uniform generation of sub-nanometer silver clusters in zeolite cages exhibiting high photocatalytic activity under visible light. ACS Applied Materials & Interfaces. 2018 Aug 6;10(34):28702-8.